GeoArabia, Vol. 3, No. 2, 1998
Gulf PetroLink, Bahrain

Sequence Stratigraphy of the Arab A to C Members and Hith Formation, Offshore Abu Dhabi

Samir R. Azer
Abu Dhabi Marine Operating Company
and Ross G. Peebles
Halliburton Energy Services

ABSTRACT

The Upper Jurassic Hith Formation and Arab members A, B and C, in central and western offshore Abu Dhabi, consist of 450 to over 600 feet of massive to interbedded anhydrites with varying proportions of limestones and dolomites. A high resolution sequence stratigraphic framework for this important petroleum reservoir interval was developed from core and well log data, and various inorganic geochemical analyses. This data was acquired from wells located at 3 locations spread over 100 kilometers. Nineteen shallowing-upward parasequences, corresponding to fourth and possibly fifth-order cycles, were recognized for the Arab members as follows: A (7 cycles), B (5 cycles), and C (7 cycles). Five parasequences were recognized for the Hith Anhydrite Formation.

The Arab parasequences are arranged in a layer-cake stacking pattern and vary in thickness from 6 to 30 feet. These are interpreted to correspond to transgressive-regressive episodes which are driven by low-amplitude sea-level fluctuations (eustacy). The typical parasequence consists of shoal grainstones, representing transgressive system tracts, that pass upward into thin-bedded lagoonal burrowed mud / wackestones, representing the maximum flooding surface. These are overlain by coarse bioclastic grainstones capped by algal laminites and culminate into supratidal anhydrites, which pinchout eastwards. In the west offshore Abu Dhabi the parasequences are thicker and consist of intertidal pack / grainstones overlain by anhydrites.

INTRODUCTION

The Upper Jurassic Arab Formation in central and western offshore Abu Dhabi (study area) contains prolific hydrocarbon-bearing zones, designated as the Arab A to D reservoirs (Figures 1 and 2). The reservoir zones consist of carbonates which are separated by anhydrite layers with the Hith Anhydrite Formation forming the uppermost regional seal. In eastern offshore Abu Dhabi, where open-shelf sedimentation developed in the Late Jurassic, the Arab zones cannot be distinguished apart, and the Hith Anhydrite passes laterally to porous lagoonal dolomites (Murris, 1980; Al-Silwadi et al., 1996).

The cyclic nature of the Arab and Hith formations lends itself to a sequence stratigraphic analysis (Vail et al., 1977). Le Nindre et al. (1990), for example, based on the integration of sedimentological, macro- and micro-fossil analysis of outcrops in central Saudi Arabia, interpreted the Arab D, C and B members, and the Arab A Member / Hith Formation as 3rd-order sequences.

The objectives of this paper are to develop a higher-order sequence stratigraphic framework for the Arab C, B and A members and Hith Formation which emphasizes cyclicity, facies architecture and diagenesis. In this study these strata are sub-divided into parasequences which correspond to 4th- and possibly 5th-order, shallowing-upward facies cycles.

Each Arab parasequence starts with a deepening component (transgressive system tract or TST), followed by a transitional maximum flooding surface (MFS), condensed section (CS), and a final shallowing component (highstand system tract or HST). The HST is further divided into an early highstand system tract (EHST) which fills the vertical accommodation space, and a progradational (regressive) late highstand system tract (LHST). The terms HST, TST, MFS and CS, which are usually applied to 3rd-order cycles or sequences, are adopted here for the higher-order parasequences.

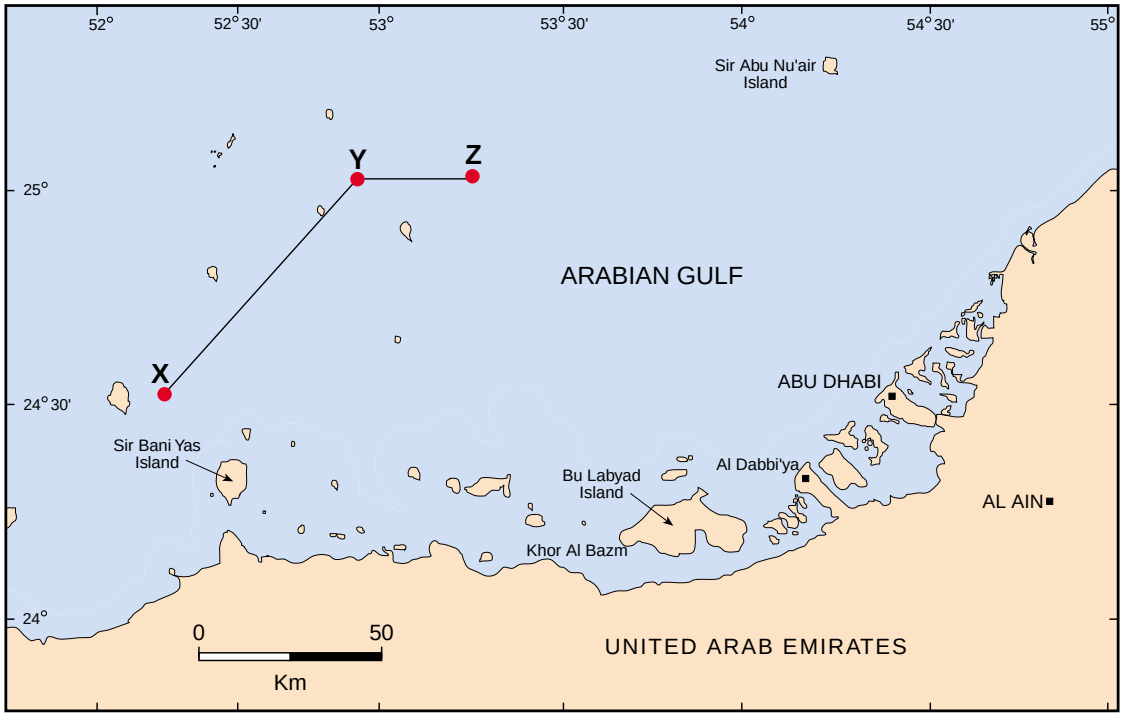

Figure 1: The study is based on 6 wells, consisting of three well-pairs each, located near sites X, Y and Z in the western and central Offshore Abu Dhabi, United Arab Emirates.

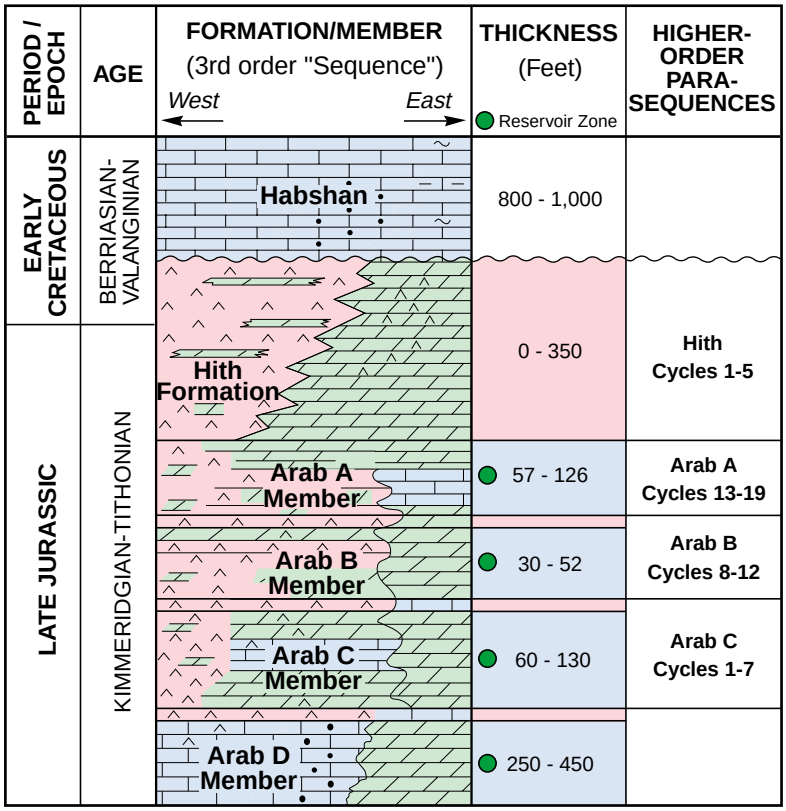

Figure 2: Lithostratigraphy and sequence stratigraphy of the Arab C, B and A members and Hith Formation suggests that the Hith/A, B and C each corresponds to a 3rd-order "Sequence". In turn these can be subdivided into higher-order "Parasequences" which correspond to shallowing-upward facies cycles.

The study is based on 6 wells, consisting of three well-pairs each, located near sites X, Y and Z (Figure 1). A total of 712 feet (ft) of core slabs and thin sections were examined. In addition, a full suite of logs was interpreted and the following geochemical analyses were performed: strontium isotopes (13 samples), sulfur isotopes (77 samples), carbon / oxygen isotopes (154 samples), scanning electron microscopy (8 samples), and x-ray diffraction (7 samples).

IDEALIZED ARAB CYCLE

Two types of shallowing-upward Arab cycles (parasequences) were recognized in this study and these can be idealized as shown in Figure 3.

Peritidal Cycle

The first parasequence corresponds to the more common peritidal cycle. The peritidal zone ranges from above the highest storm or spring tides to below the lowest tides. These parasequences range in thickness from 3 to 18 ft. Their base usually consists of a basal thin transgressive lag deposit containing micritic intraclasts and a bioclastic, micropeloid dolo-packstone / grainstone with occasional discrete anhydrite nodules (TST). The TST deposit is overlain by a thin, dense-bedded to nodular sub-aqueous anhydrite deposited in lagoonal waters (CS). This is followed by mollusk, pellet grainstone with occasional cross-bedding and scour horizons gradually passing upward, in parts, to stromatolite bindstone (EHST). The cycle terminates with a nodular to bedded anhydrite cap (LHST).

Shallow Subtidal Cycle

The second kind of parasequence corresponds to the shallow subtidal cycle. It consists of muddy limestone overlain by more grainy facies with an erosional top. The parasequence commences (TST) with bioturbated, wavy-laminated, worm-burrowed dolo-mudstones with gypsum pseudomorphs (rosettes and blades) capped by a dense laminated bored MFS. The regressive phase (HST) is represented by an intraclast, mollusk, grainstone / rudstone topped by an exposure surface.

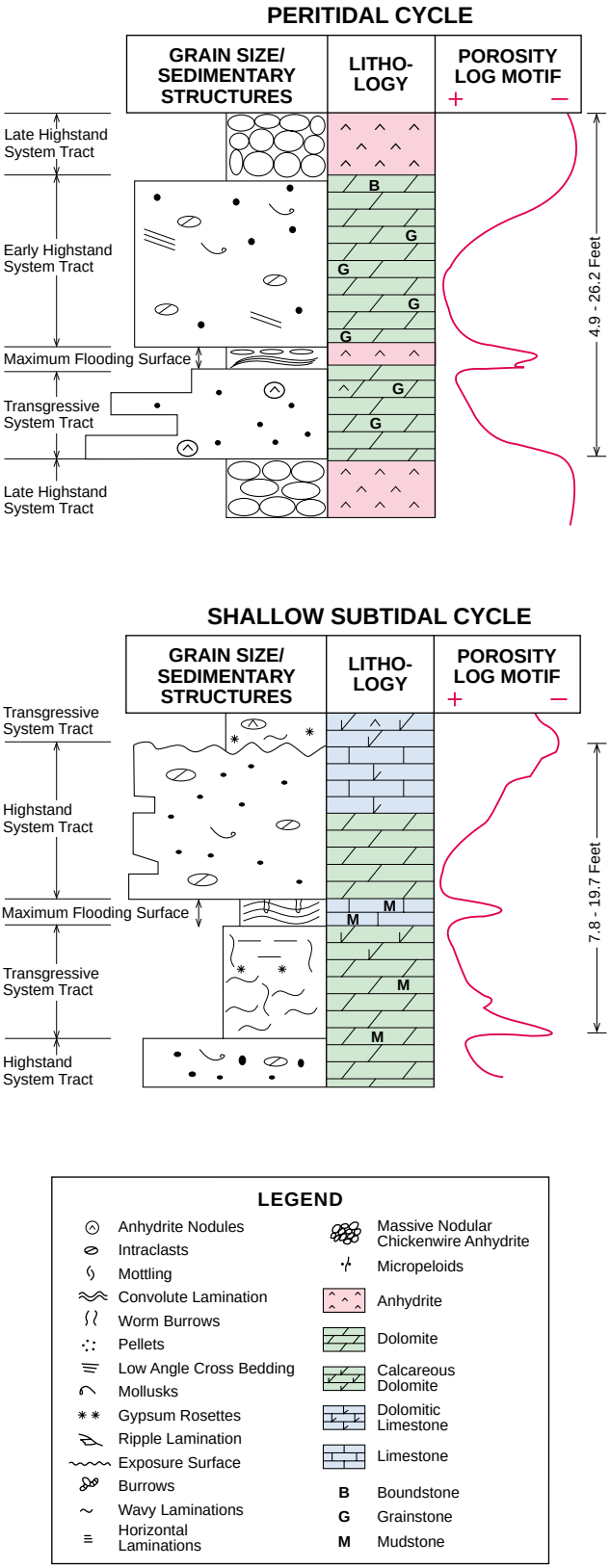

Figure 3: Idealized types of Arab parasequences correspond to the peritidal cycle, or the less common shallow subtidal cycle.

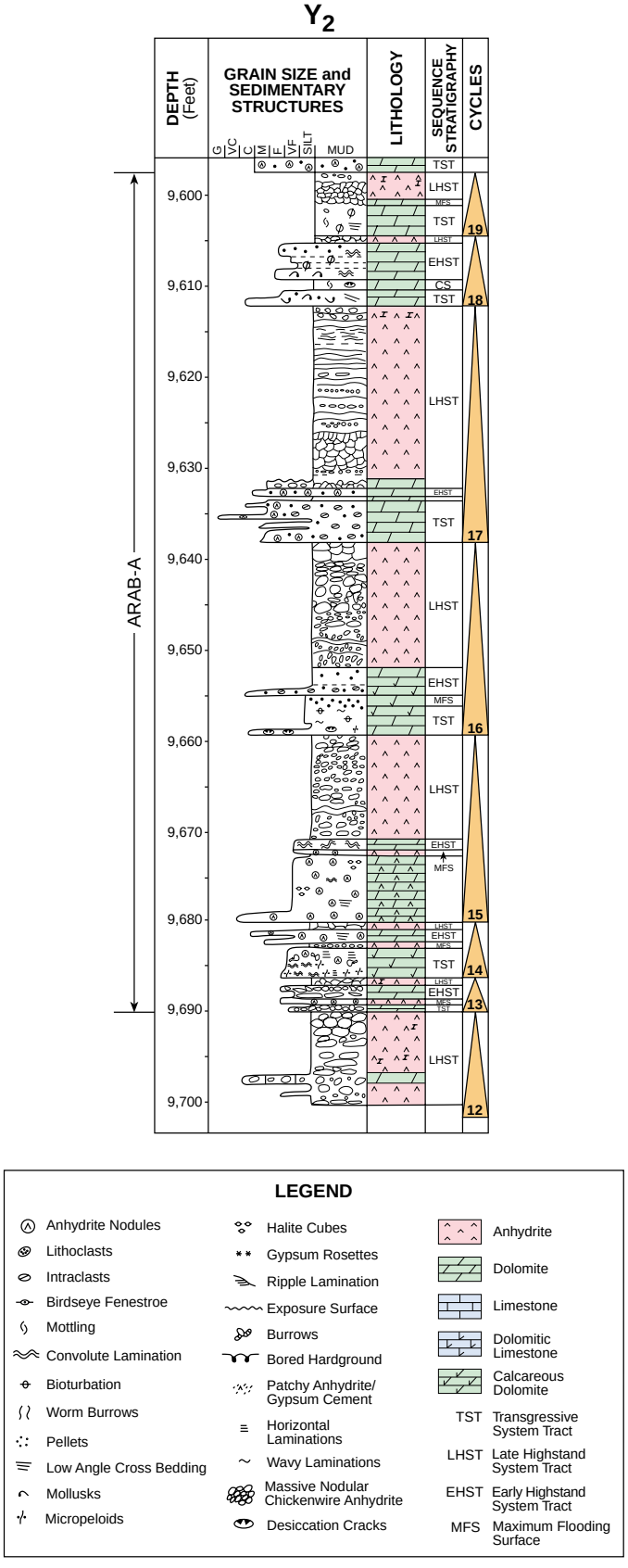

Figure 4: Arab Cycle Stacking Patterns from wells Y_1 and Y_2 show the sedimentary structure of the 19 parasequences (4th and ?5th-order cycles) of the Arab A, B and C members.

TRANSGRESSIVE-REGRESSIVE COMPONENTS

The Arab parasequences generally have a shallowing-upward trend consisting of transgressive - regressive components. Most of the sediment in the parasequence is deposited during the highstand regressive interval (Tucker, 1993). The Arab parasequences and their sedimentary petrology is depicted for composite well Y in Figures 4 and 5.

Transgressive (TST) Component

The transgressive component (TST) of the Arab parasequences shows relatively deeper facies (subtidal - lower intertidal) accompanied by common horizontal to low-angle laminations, burrows, bioturbation, mottling, micropeloids, intraclasts, discrete anhydrite nodules and gypsum rosettes. Occasionally a dense bored hardground or dolomite crust caps the TST. A lag deposit sometimes occurs at the base. The TST facies are often heterogeneous and composed of several facies of varying thickness, resulting in an irregular distribution of porosity and permeability.

Petrographically, the transgressive component mainly exhibits marine diagenetic textures (Figure 5), micritization of the matrix / grains, isopachous cements, increased dolomitization and occasionally abundant ostracods. The basic pore types associated with the TST are intercrystalline, and to a lesser extent, matrix and rarely moldic. Log curve shapes of the TST generally show a bell-shaped motif, characteristic of transgressions.

Regressive (HST) Component

The highstand or regressive component (HST) shallow-upwards and include intraclasts, mollusks, pellets, ripple laminations, scour surfaces, algal laminations and occasional erosional surfaces. Often they are capped by bedded, nodular anhydrites representing the LHST. The HST grainstones are typically more homogenous than those of the TST and less muddy, thus having higher porosity and permeabilities.

Petrographically, the regressive parts demonstrate a greater extent of surface-related diagenesis than those of the TST (Tucker, 1993). They generally have a more grainy facies (intertidal) and are characterized by pellets, mollusks, algae, increased anhydritization and extensive leaching. The HST shows the best reservoir characteristics with intergranular, moldic and vuggy pore types. Vadose compaction and meteoric cements are sometimes observed. Log curves of the HST generally show a cone shaped regressive log motif.

PARASEQUENCE BOUNDARIES

Several exposure surfaces occur throughout the Arab parasequences. Where the cycle is incomplete, eroded crusts or surfaces occur at the top of the EHST, with no anhydrite caps. More complete cycles show exposure surfaces either: (1) towards or at the top of the EHST; or (2) iron-stained anhydrite tops with undulated contacts.

Some of these exposure surfaces, which occur in the lower Arab C Member, correlate from well to well (Figure 6). Some of these surfaces are associated with extensive dissolution. These localized exposure surfaces can be considered as parasequence boundaries due to their limited lateral extent. Hardgrounds occur at cycle tops or as bored hardgrounds representing the MFS.

CONDENSED SECTIONS AND MAXIMUM FLOODING SURFACES

The CS / MFS is manifested in six forms in the Arab A, B and C parasequences (4th and ?5th-order cycles). These forms are:

(1) nodular anhydrite,
(2) wavy laminated anhydrite,

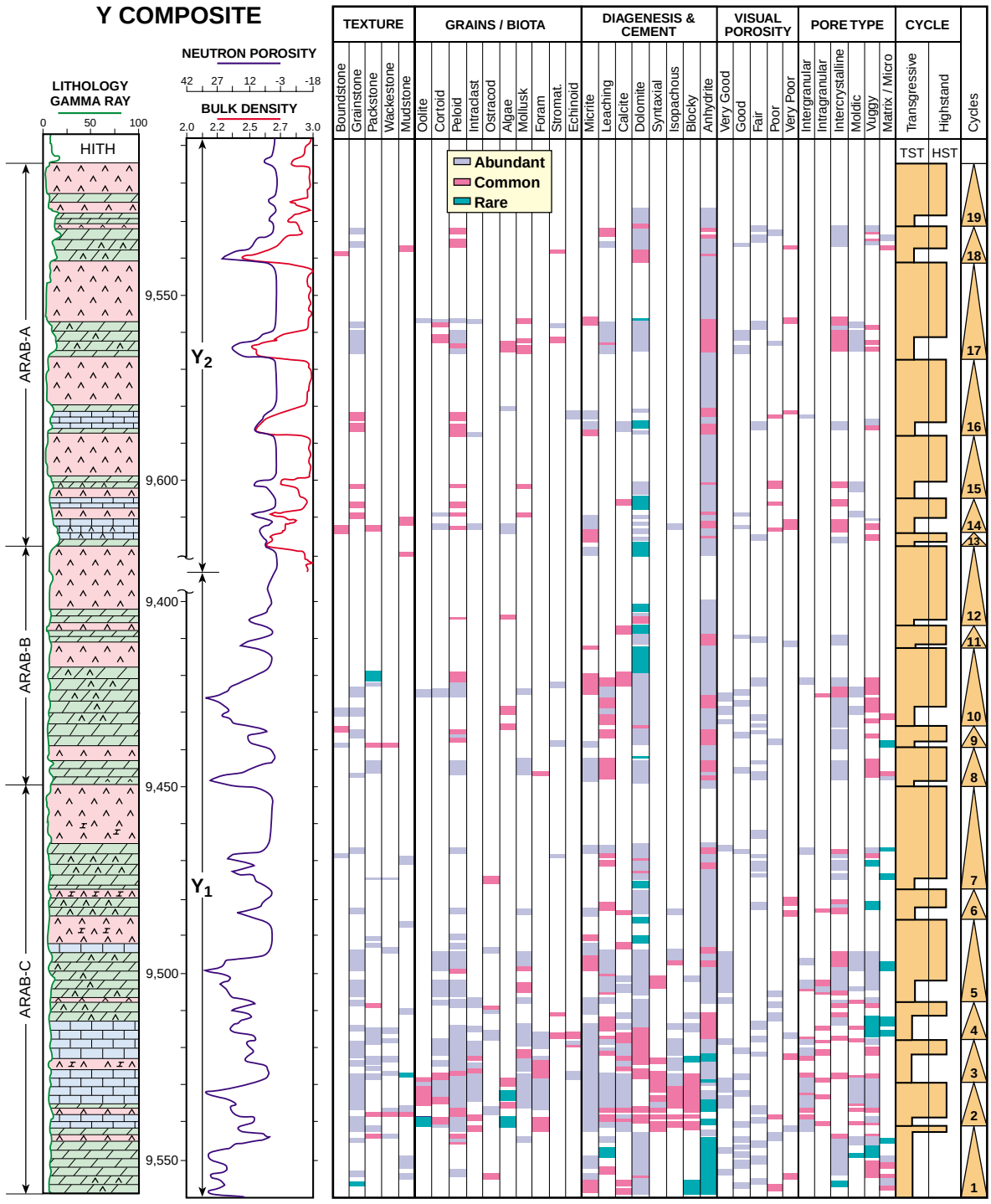

Figure 5: Sedimentary petrology at site Y.

(3) bored hardgrounds,
(4) dense laminated lime-mudstones or sucrosic dolomites,
(5) gypsum blades and rosettes, and
(6) burrow-mottled facies.

These CS / MFS forms range from 2 inches to 1.5 ft in thickness and are sometimes not apparent on logs. Generally they appear as dense spikes on porosity logs with corresponding shaley spikes on the gamma ray log curve. In Figure 6 these features can be correlated between wells at sites X, Y and Z, although the facies of the CS / MFS change between the locations.

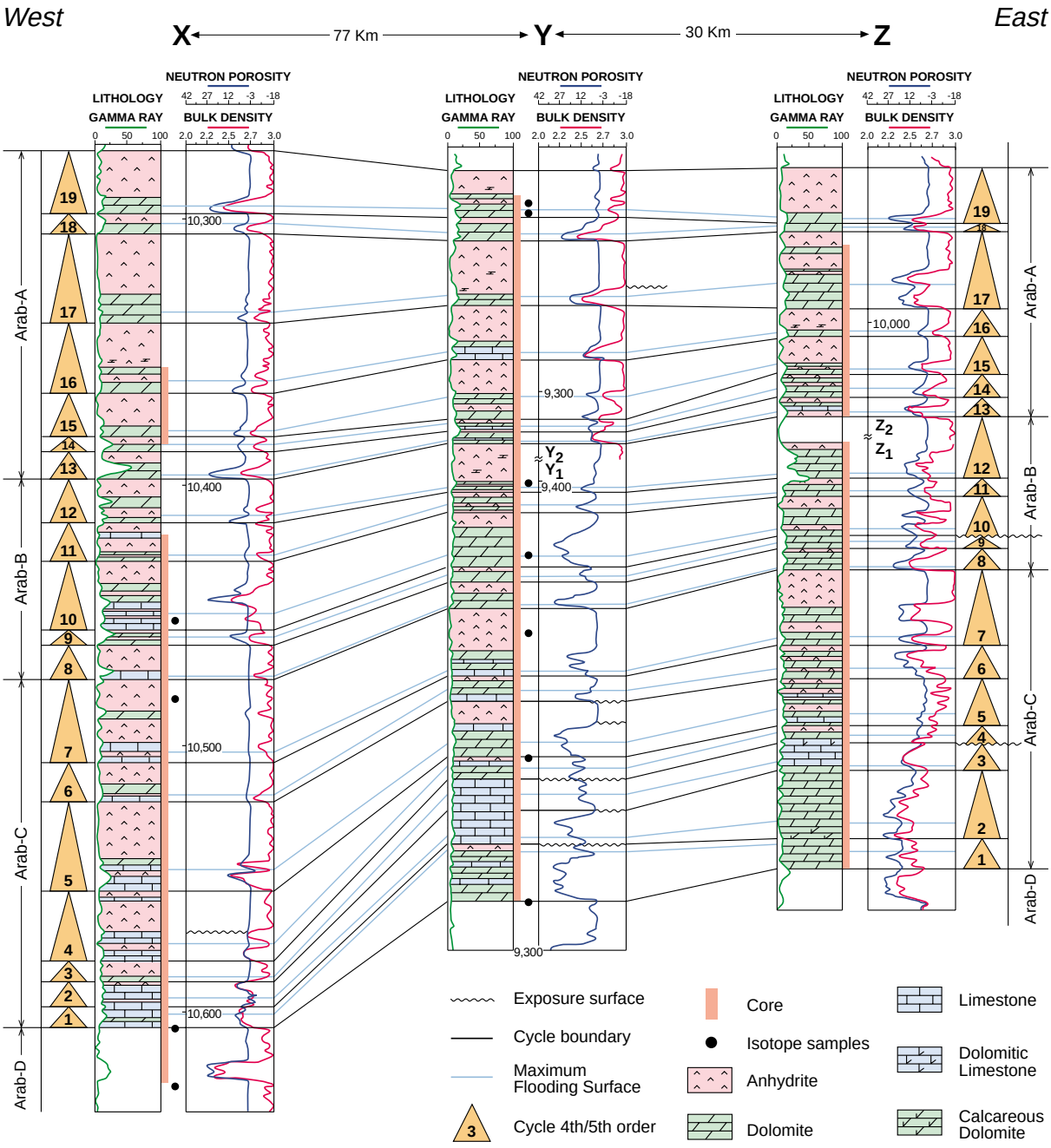

Figure 6: Correlation of Arab Cycles from wells at locations X, Y and Z indicates good correlation of the parasequences over a distance of over 100 kilometers.

The CS / MFS generally corresponds with low porosity / low permeability and can constitute a vertical permeability barrier. As a result, magnesium-rich fluids are trapped below the MFS enhancing dolomitization processes in the underlying TST.

The thin anhydrites (CS) are discontinuous lensoid bodies that may be in the order of tens of kilometers in lateral extent. Since they lack typical sabkha evaporite characteristics, such as crystal morphology, the anhydrites may have originated by the replacement of gypsum deposited in salt basins (La Pointe et al., 1990). The presence of restricted marine fauna, together with the absence of open marine fauna in the Arab carbonates, also suggests that the evaporites formed sub-aqueously in large hypersaline, coastal lagoons and ephemeral lakes (Peebles et al., 1995) and not in a sabkha environment.

ARAB CYCLES

In the studied cores very few facies are similar to the present Abu Dhabi sabkha environment, which consists of carbonate sand / grainstones with enterolithic and anhydrite nodules. All facies observed in core appear to be very shallow inner shelf facies. The TST are often rich in intraclasts or fecal pellets reworked from a tidal flat, implying flooding over this uppermost intertidal facies. The mollusk grainstones (both TST and HST) usually have a very low diversity fauna typical of high salinity, harsh environments.

The fauna themselves are high salinity tolerant types (high-spired gastropods, small bivalves). These grainstones could represent lagoonal shoals or uppermost intertidal beach deposits (cheniers / beach ridges). The CSs are interpreted as the result of deepening and restriction in very saline, very shallow waters (unfossiliferous mudstones, thin evaporites). The LHST sulphates may have formed sub-aqueously in cut-off lagoons that evolved to ephemeral ponds.

Arab C Cycles

The Arab C consists of three major carbonate facies; namely: (1) oolitic skeletal grainstones, *Favreina*, *Prethecoprolithus* pelletal grain / packstones; (2) ostracod lime-mudstones, and (3) algal limestones with *Clypeina* sp. (de Matos, 1994). The Arab C Member in well Y_1 is 111 ft thick. It thins gradually from west to east to a zero line nearly coincident with the Hith edge (de Matos, 1994; Al-Silwadi et al., 1996).

The base of the Arab C Member is an iron-stained unconformity surface and the contact occurs between its basal dense lime-mudstones and the underlying large, flattened anhydrite nodules, which cap the Arab D Member. In location X, the base Arab C is a sharp contact between the transgressive, coarse-grained intraclast floatstone and the underlying vertically-aligned anhydrite with an algal mat. In location Z, the base of the Arab C Member is questionable but possibly corresponds to an erosional surface with karst.

As seen in Figure 4, the Arab C Member (Arab C Zone and the overlaying Arab C Anhydrite) is composed of 7 shallowing-upward parasequences (4th and ?5th-order cycles) described here in ascending order.

Cycle 1 commences with burrowed and burrow-mottled, laminated, sucrosic dolomite with gypsum pseudomorphs with good intercrystalline porosity (TST), overlain by one foot of dense, nodular, contorted, layered anhydrite (CS), and cross-stratified, micro-peloid sucrosic dolo-grainstone (HST) capped by an eroded dolomite crust.

Cycle 2 starts with a burrowed, anhydritic dolo-mudstone / wackestone (TST), with a strongly-bored hardground at its top (MFS). The HST is a coarsening-upward, medium to poorly-sorted, peloid, mollusk grainstone / rudstone capped with an irregular eroded surface.

Cycle 3 starts with a laminated, anhydritic dolomite with abundant gypsum rosette pseudomorphs, overlain by an intraclast floatstone grainstone. The CS is 3-inches thick and composed of a dense, lime-mudstone, bounded by micro-stylolites. The HST is made up of three fining-upward cycles of cross-stratified peloid, mollusk grainstone. Each fining-upward cycle begins with a scour surface. The HST is capped by a cemented hardground.

Cycle 4 commences with mottled stratified, micro-peloid, sucrosic dolo-grainstone capped by a strongly-burrowed peloid pack / wackestone (CS). An EHST is composed of pellet intraclast dolo-packstone, capped by nodular chicken-wire anhydrite (LHST).

Cycle 5: The TST of this cycle is a pellet intraclast anhydritic dolo-grainstone capped by a 3-inch, dense, bored mudstone, capped by an interpreted exposure surface (CS). The EHST is a dolomite with anhydrite, gypsum and halite cubes. The LHST is a nodular anhydrite with an erosional surface.

Cycle 6: The basal flooding in this cycle is associated with micritized peloid dolo-grainstone capped by a one-foot dolomitic anhydrite (CS). The EHST is an anhydritic dolomite with irregular laminae, scour horizons and halite pseudomorphs. The LHST is a nodular anhydrite.

Cycle 7 is the uppermost cycle of the Arab C Member. It begins with a dolo-mudstone with gypsum pseudomorphs, grading upward to intraclast dolo-floatstone, capped by a bioturbated dolomite with flattened anhydrite nodules (CS). The EHST commences with a ripple-laminated micro-peloid dolo-grainstone, which passes upward into stromatolitic bindstone. This is overlain by a pellet anhydrite dolo-grainstone and capped by more than 15 ft of nodular, bedded enterolithic anhydrite (LHST).

Arab B Cycles

Five 4th and ?5th-order cycles comprise the Arab B Member (52 ft thick) as follows:

Cycle 8: The basal Arab B TST is a peloid intraclast packstone capped by a 2-inch dense dolomite (CS). The EHST is a cross-bedded peloid, mollusk, dolo-grainstone, packstone overlain by a bedded contorted LHST anhydrite.

Cycle 9 commences with a stromatolite bindstone capped by a very thin laminated dolo-wackestone (CS). The EHST is an intraclast dolo-packstone overlain by nodular anhydrite (LHST).

Cycle 10 starts with alternating dolo-mudstone, intraclast packstone passing upward to anhydrite intraclast pellet grainstone capped by a dense, olive-green, sucrosic dolomite (CS). The overlaying EHST is a cross-bedded pellet dolo-grainstone passing upward into a ripple laminated anhydritic dolomite capped by a LHST nodular to bedded anhydrite.

Cycle 11 begins with a peloid dolo-packstone, laminated mudstone capped by a thin layer of nodular anhydrite (CS). The EHST is a laminated anhydritic dolo-packstone capped by a nodular anhydrite (LHST).

Cycle 12: The uppermost cycle of the Arab B Member commences with an intraclast pelecypod grainstone capped by a 4-inch wavy laminated anhydrite (CS). The EHST is a mollusk, peloid dolo-grainstone with scoured horizons, capped by a thick nodular anhydrite (LHST).

Arab A Cycles

The Arab A Member is approximately 90 ft thick and is composed of 7 cycles (Figures 4, 5 and 6), which are, in part, characterized by thicker supratidal anhydrite caps.

The lowermost **Cycles 13, 14** and **15** differ in thickness but commonly begin with a laminated, highly-bioturbated, burrowed, anhydritic peloid dolo-packstone / wackestone capped by thin anhydrite beds (CS). The EHST are composed of peloid, intraclast, rippled grainstone / packstone, sub-ordinate boundstone capped by nodular anhydrites (LHST).

Cycle 16 commences with intraclast floatstone, fining-upward to laminated peloid grainstone, capped by a thin layer of gypsum blades and rosettes (CS). The EHST also fines upward from peloid intraclast dolo-grainstone to dense peloid grainstone capped by LHST nodular anhydrite.

Cycle 17 starts with fining-upward sub-cycles of pellet intraclast grainstones, capped by a dense muddy dolomite (CS). The EHST is an intraclast dolo-grainstone capped by anhydritic dolo-grainstone with an iron-stained exposure surface. The LHST is a nodular and bedded anhydrite.

Cycle 18 begins with an intraclast mollusk dolo-packstone, capped by a 1.5-inch mottled stromatolite boundstone with fenestrae (CS). The EHST is a pelletal dolo-grainstone, capped by a thin black organic-rich microbial mat, overlain by nodular, bedded anhydrite (LHST).

Cycle 19: The uppermost cycle of the Arab A Member commences with laminated bioturbated, mottled dolo-mudstone (TST and CS), capped by a nodular anhydrite mosaic (LHST).

HITH CYCLES

The top of the Hith Formation is a sharp boundary on the wireline logs, indicating the abrupt change from massive Hith anhydrites to the carbonates of the overlying Habshan Formation. Five Hith parasequences (4th and ?5th-order cycles) can be correlated between all three locations (Figure 7).

The parasequences were defined based on wireline logs, since cores were not available. The Hith cycles thin progressively from west to east due to the thinning of anhydrites in that direction reaching zero thickness in the east central part of the study area. A decrease in accommodation space (HST) is noted from Hith Cycle 1 to Hith Cycle 3 followed by flooding (Hith Cycle 4). A second relative sea-level fall occurs towards the top of the Hith Formation.

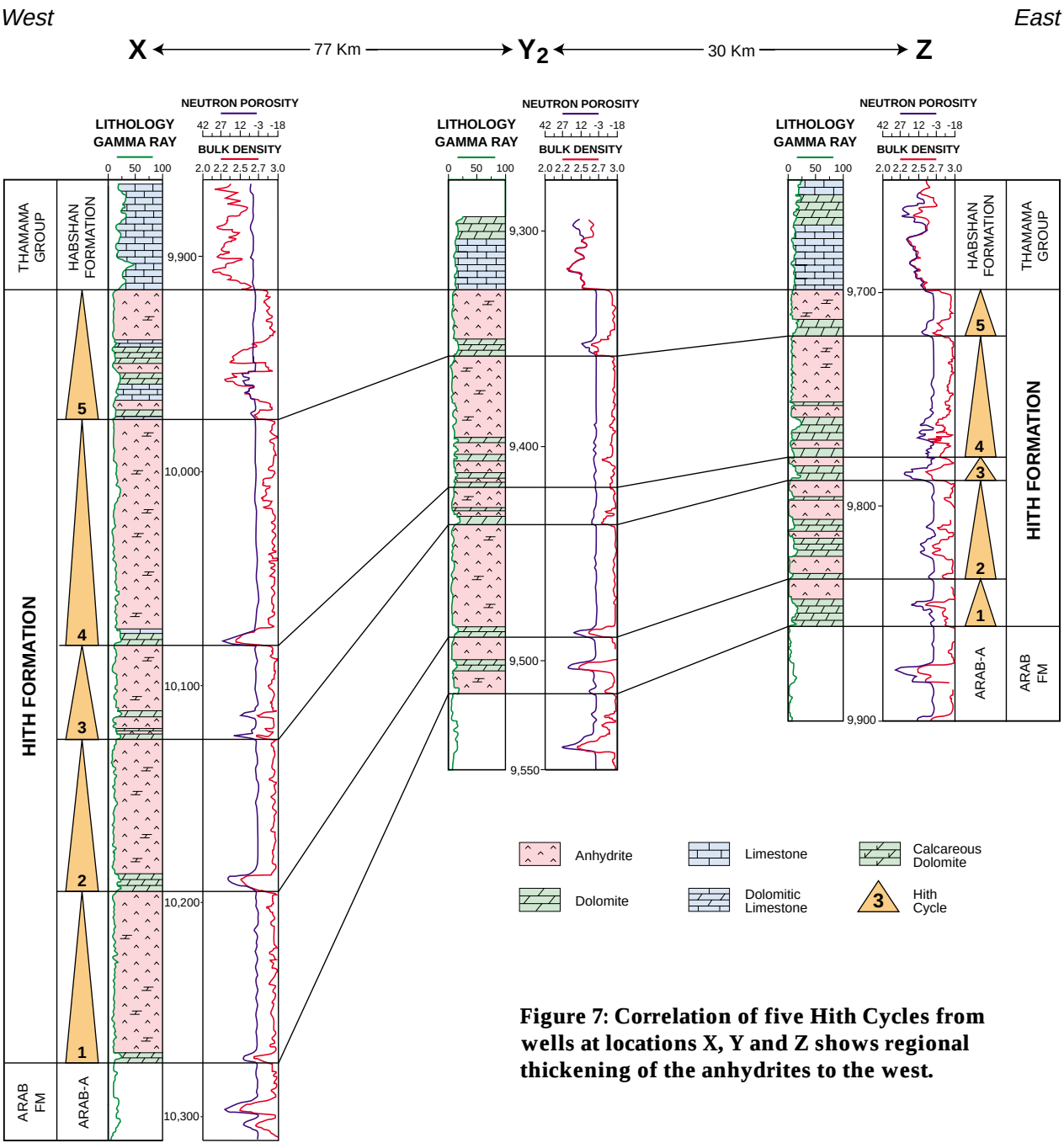

Figure 7: Correlation of five Hith Cycles from wells at locations X, Y and Z shows regional thickening of the anhydrites to the west.

ARAB CYCLE STACKING PATTERNS - FISCHER PLOTS

Fischer plots can be used to show variations in 3rd-order accommodation space that reflect the systematic shifts of higher-order (4th and ?5th-order) cycle thicknesses (Goldhammer et al., 1993). In the case of the Arab A, B and C members the stacking patterns of the parasequences mirror the longer-term 3rd-order relative sea-level curve (Figure 8). In location Y, the 19 cycles total 266.6 ft in thickness, with an average thickness of 14 ft per cycle. In location X, the 19 cycles total 332.5 ft in thickness with an average thickness of 17.4 ft per cycle.

The Fischer plots (Figure 8) for the Arab cycles in locations X and Y show six major accommodation events, assuming constant sedimentation rates and equal duration for each cycle. A fairly good correlation exists between the Fischer plots of locations X and Y, however the 3rd-order events in the well at location X are more pronounced.

The cycle thickness illustrates that most of the upper Arab deposition was associated with highstands or regressive events. The accommodation space is driven by the proportion of sulphates and carbonates (Figure 8).

Lithostratigraphic correlation of the upper Arab members is generally fairly difficult since the anhydrites are usually discontinuous and occasionally replaced by dolomites towards the east. They can be more easily correlated based on cycle stacking patterns.

Low amplitude sea-level fluctuations and subsidence, in addition to sedimentation rate and depositional facies drive the upper Arab cyclicity. The similarity of the Fischer plots at locations X and Y, which are 77 km apart, suggests eustatic control. The Arab parasequences are interpreted to reflect relative sea-level changes in the order of ten feet, whereas the 3rd-order Arab members might correspond to relative sea-level changes of the order of several tens of feet.

CARBON/OXYGEN ISOTOPE ANALYSIS

Seventy-six carbonate and seventy-eight evaporite (sulphate) samples were analyzed for $\delta^{13}C$ and $\delta^{18}O$ values (Figure 9). The results show a moderately close grouping in the second quadrant and slightly into the first. This reflects the mostly positive to slightly negative range of the $\delta^{18}O$ values and the strongly positive $\delta^{13}C$ values. The average $\delta^{18}O$ values are 1.3‰ for dolomite and 2.2‰ for sulphate while the average $\delta^{13}C$ value is 6.7‰ for both dolomite and sulphate.

These values are significantly more positive than the normal marine values for the Upper Jurassic (Allen and Wiggins, 1993; Hosler et al., 1988). The positive or heavy $\delta^{18}O$ values suggest dolomitization and sulphate precipitation from evaporation-concentrated brine at low temperatures. The strongly positive or heavy $\delta^{13}C$ values are the result of bacterial or microbial methane production that releases large amounts of isotopically heavy CO_2 which results in pore waters with heavy $\delta^{13}C$ values. As microbial methane usually forms shallower than one kilometer depth, the heavy $\delta^{13}C$ values seen here imply shallow burial dolomitization and shallow burial diagenetic alteration of the evaporites (Allen and Wiggins, 1993).

Together, the $\delta^{13}C$ / $\delta^{18}O$ values suggest shallow burial diagenetic alteration of evaporites and seepage-reflux dolomitization in the shallow subsurface. The reflux is believed to be driven by falls in relative sea-level (lowstands), which cause the shallow dolomitizing pore fluids (groundwater) to quickly pass through and dolomitize the underlying units. Shallow burial dolomites should be stratigraphically concordant, and have generally good porosity and permeability (excluding the effect of deep burial cements such as anhydrite and saddle dolomite). Burial dolomites are generally stratigraphically discordant and destroy porosity.

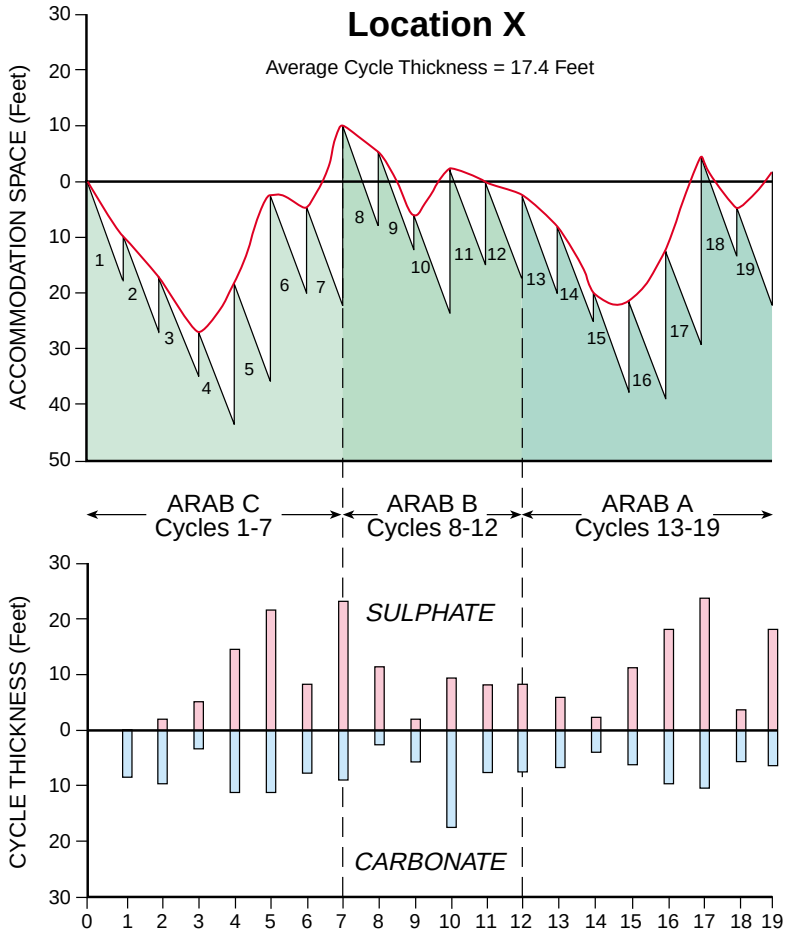

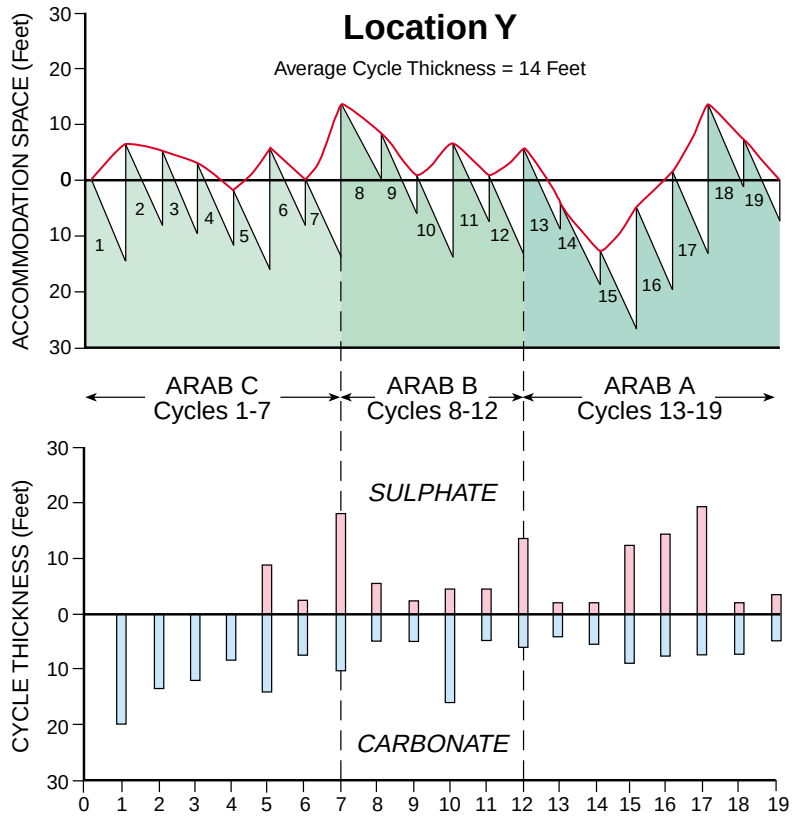

Figure 8: Fischer accommodation plots for wells located at sites X and Y are shown in the respective upper diagrams. A fairly good correlation exists between the wells at the two locations X and Y. In the lower respective diagrams the accommodation space is driven by the proportion of evaporites (sulphates) and carbonates.

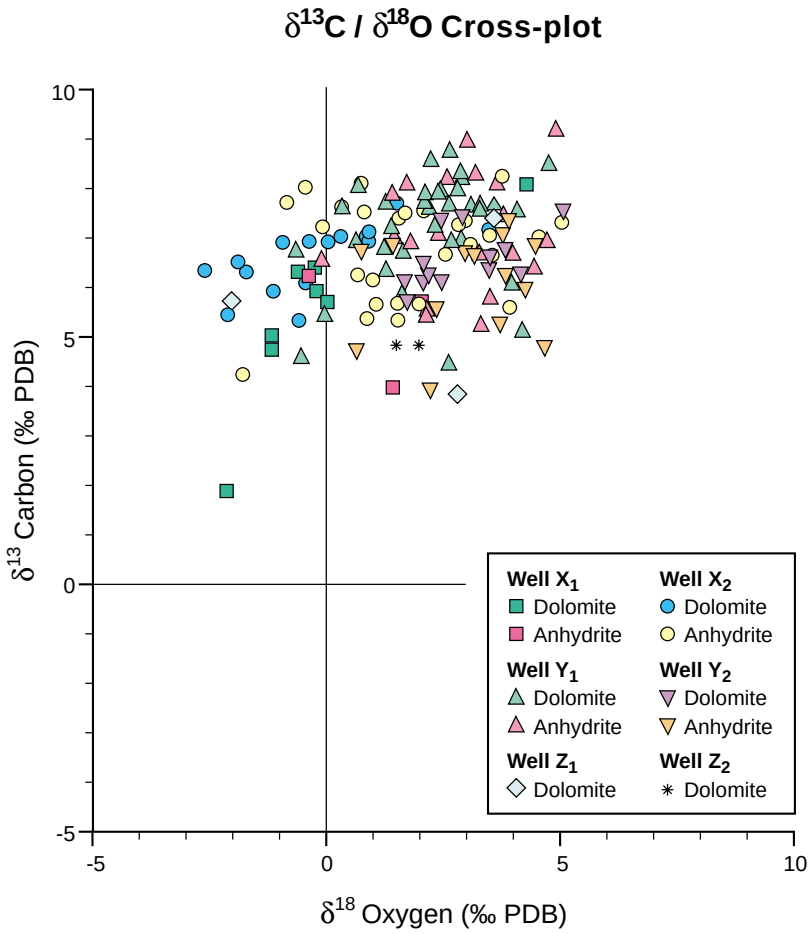

Figure 9: Carbon/ Oxygen isotope cross-plot of 76 carbonate and 78 evaporite (sulphate) suggests dolomitization and sulphate precipitation from evaporation-concentrated brine at low temperatures.

The Upper Jurassic Smackover (US Gulf Coast), Upper Permian Zechstein (Northern Europe) and Permian San Andres (Permian Basin) dolomites, all have a $\delta^{13}C$ / $\delta^{18}O$ signature similar to that observed in the Arab Formation and all have been interpreted as the result of seepage-reflux dolomitization (Tucker and Wright, 1990; Moore, 1989).

SULPHUR ISOTOPE ANALYSIS

Seventy-seven evaporite samples were analyzed for $\delta^{34}S$ content and the results ranged from 15.8‰ to 19.8‰ with an average value of 17.6‰. The $\delta^{34}S$ analysis provided both sedimentologic and stratigraphic information. Sedimentologically, it was seen that the $\delta^{34}S$ value gradually decreased upsection in thick (>10 ft) continuous evaporite intervals and commonly had a distinct high at the top of the interval. This high alteration was not found at the top of all thick evaporite intervals.

The $\delta^{34}S$ value is derived from the ratio of $\delta^{34}S / \delta^{32}S$ isotopes. This ratio is determined by the relative proportions of organically-derived (bacterial reduction) sulphur which is "enriched" in the ^{32}S isotope and inorganic (oxidized) sulphur which is "enriched" in the ^{34}S isotope. In increasingly restrictive conditions in a maturing evaporite basin, reducing conditions will concentrate the ^{32}S isotope, thus decreasing the $^{34}S / ^{32}S$ ratio or $\delta^{34}S$ value. This supports an evaporite depositional model in which a hypersaline lagoon matures or evolves into a hypersaline lake or ephemeral pond.

In a sequence stratigraphic perspective, as the highstand portion of the depositional cycle consumes its vertical accommodation space and begins to prograde seaward it leaves behind a restricted, "cut-

off" basin that receives ever-diminishing supplies of marine recharge and becomes increasingly evaporative. In this depositional scenario the lagoon evolves into a hypersaline lake (salina) which may further evolve into a sabkha before the marine flooding that starts the overlying cycle. When this next cycle floods the area, the upper portion of the underlying evaporite is diagenetically altered by the new oxygen-rich marine pore water. This new pore water possesses a higher $^{34}S/^{32}S$ ratio and produces a high ^{34}S value in the altered evaporites at the top of the interval.

Stratigraphically, the $\delta^{34}S$ values are typical of Late Jurassic values (16-19‰) reported by Claypool et al. (1980). The $\delta^{34}S$ stratigraphy is shown in the table below:

Table 1

Zone	$\delta^{34}S$(‰) (average)	Number of samples
Arab A	17.3	19
Arab B	17.6	16
Arab C	17.7	43

The stratigraphic resolution of $\delta^{34}S$ values is generally assumed to be only 1-2‰ (W. Hosler, personal communication 1995). Therefore, the very small differences between the average $\delta^{34}S$ values of the Upper Jurassic Arab members cannot confidently be attributed to stratigraphic position or age. However, the global sulphur curve does show a trend of decreasing values from the Upper Jurassic to Lower Cretaceous as seen in Figure 9 of Claypool et al. (1980).

STRONTIUM ISOTOPE STRATIGRAPHY

Thirteen anhydrite and dolomite samples were collected from the Hith and Arab members. These were analyzed for Strontium Isotope $^{87}Sr/^{86}Sr$ ratios (Figure 10). A 3-D cross-plot of $\delta^{13}C$, $\delta^{18}O$ and $^{87}Sr/^{86}Sr$ ratio (Figure 11) revealed very similar isotopic signatures except for one sample. This sample is a clay-rich dolo-mudstone and the alumino-silicate clays are known to elevate strontium ratios (Allen and Wiggins, 1993).

As strontium isotope samples show a similar isotopic signature, they are probably derived from pore fluids with similar characteristics, i.e. a common strontium reservoir under similar pore fluid conditions. The strontium stratigraphy of the Hith-Arab interval studied is summarized in Table 2.

Table 2

Rock Unit	$^{87}Sr/^{86}Sr$ Ratio (average)	Age[1]	Number of samples
Hith (base)	0.707019	Early Tithonian	1
Arab A	0.706972	mid-Late Kimmeridgian	1
Arab B	0.706974	mid-Late Kimmeridgian	4
Arab C	0.706964	mid-Late Kimmeridgian	3
Arab D (top)	0.706959	mid-Late Kimmeridgian	2

[1] Age determinations based on the Strontium seawater curves of Smalley et al. (1989), Koepnick et al. (1990) and the proprietary, unpublished Arabian Seawater Curve developed by Halliburton.

The age assignments shown above are in agreement with the sequence stratigraphic framework defined by Le Nindre et al. (1990).

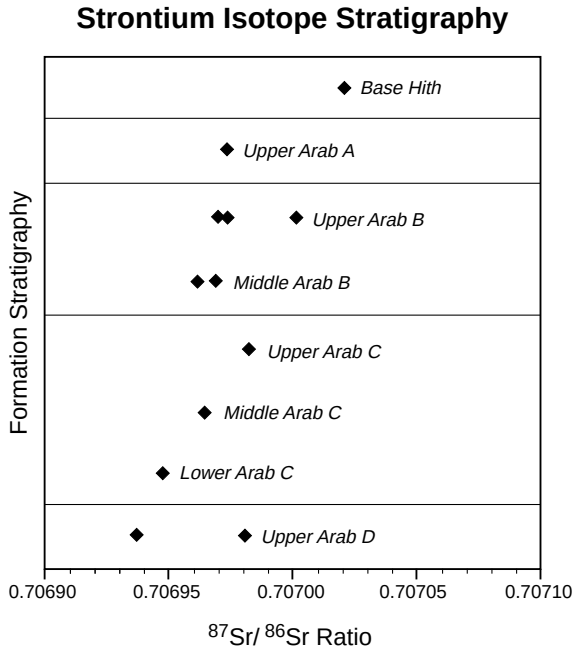

Figure 10: Strontium Isotope Stratigraphy for 12 anhydrites and dolomites which are used in the 3-D cross-plot in Figure 11.

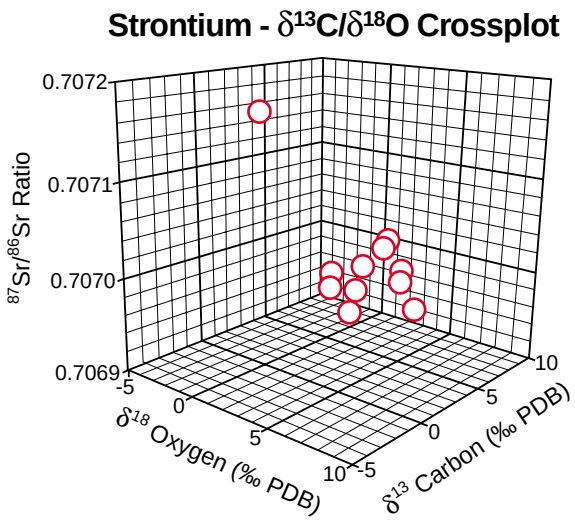

Figure 11: A 3-D cross-plot of Strontium ratio (Figure 10) to Carbon and Oxygen isotopes (Figure 9) show a similar isotopic signature for the anhydrites and dolomites indicating they are probably derived from a common strontium reservoir under similar pore fluid conditions.

The small differences between the $^{87}Sr/^{86}Sr$ ratio values for the Arab members fall within the ±0.00001 range of error and cannot therefore be attributed to stratigraphic age. The great similarity suggests that the dolomites and evaporites formed at nearly the same time and / or from a pore fluid having the same reservoir of strontium. It is likely that during shallow burial diagenesis, evaporite-rich pore waters from the upper Arab members were co-mingled to produce a nearly homogenous strontium isotope signature for the upper Arab members. This implies shallow burial alteration of the evaporites and shallow burial dolomitization of the carbonates.

X-RAY DIFFRACTION ANALYSIS

Seven dolomite samples underwent X-Ray Diffraction (XRD) analysis to determine their ordering and stoichiometry. A cross-plot (Figure 12 and Table 3) of dolomite order ratio and mole % $CaCO_3$ reveals the EHST dolomites to be very similar while the TST dolomites are heterogeneous. The EHST dolomites are all pellet dolo-grainstones and have an average order ratio of 0.78 and an average mole % $CaCO_3$ of 49.60%.

The moderate to well-ordered state of these dolomites and their similar stoichiometric nature (nearly 50-50% Ca and Mg ratio) suggests that these dolomites formed during shallow burial diagenesis in the presence of evaporites (Tucker and Wright, 1990; Morrow, 1982). All of these dolomites have ghost fabrics (pellet grainstones) indicating replacement and all are overlain by thick anhydrite intervals. The TST dolomites have heterogeneous ordering and stoichiometry implying a variety of modes of formation.

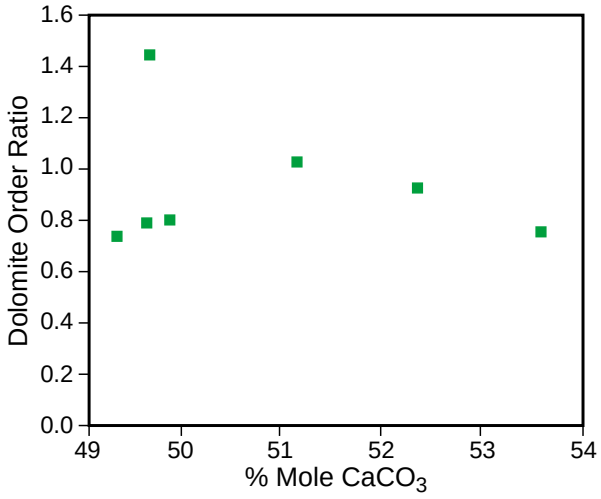

Figure 12: A cross-plot of dolomite order ratio and mole % $CaCO_3$ for 7 samples reveals the early highstand system tract (EHST) dolomites are similar while the transgressive system tract (TST) dolomites are heterogeneous. The moderate to well-ordered state of these dolomites and their similar stoichiometry suggests that they formed during shallow burial diagenesis in the presence of evaporites.

Table 3

Well	Depth (Feet)	Formation	Description	%$CaCo_3$	Ordering	Cycle Component
Y2	9,633	Arab A	Pellet intraclast dolograinstone/dolopackstone	51.14	1.03	TST
Y2	9,681	Arab A	Peloid intraclast dolograinstone/dolopackstone	49.87	0.80	Early HST
X1	9,674	Arab A	Dolomudstone	53.58	0.76	TST
Y1	9,503	Arab B	Peloid dolograinstone	49.32	0.74	Early HST
Y1	9,505	Arab B	Idiotopic dolomite	52.35	0.93	Condensed Section
Y1	9,508	Arab B	Intraclast pellet dolograinstone	49.62	1.44	TST
X2	10,688	Arab C	Pellet dolograinstone	49.62	0.79	Early HST

SCANNING ELECTRON MICROSCOPE ANALYSIS

Eight dolomite samples were examined using the Scanning Electron Microscope analysis. Dolomite was found to be in the form of well-developed, medium crystalline (50-150 mm) rhombohedrons with smooth surfaces. The same type of dolomite was present in LHST, EHST, CS and TST dolomites. The shape and size of the dolomite crystals further supports the idea of shallow burial (seepage-reflux) dolomitization. Also of note was the presence of aluminosilicate clays in small quantities in the TST dolomites only. Late burial gypsum cements were present as large bladed crystals in EHST dolomites underlying evaporite (LHST) intervals.

CONCLUSION AND RECOMMENDATION

In this study we identified 19 parasequences which correspond to fourth and possibly fifth-order cycles in the Arab A, B and C members. Arab parasequences consist of transgressive retrogradational and regressive progradational deposits, which are separated by thin, discrete condensed sections. Five additional parasequences were interpreted in the Hith Anhydrite Formation. All 24 cycles were correlatable between three sites located about 100 km apart. These correlations were further facilitated utilizing Fischer plots indicating that the Arab cycles can be attributed to eustatic sea-level fluctuations.

The sequence stratigraphic framework erected in this paper should be investigated regionally. Do the Arab and Hith formations in other regions of the Arabian Gulf consist of a similar number of parasequences?

The implications of this framework on reservoir characterization and dynamic simulation should also be considered. The spatial dimensions, geometry and orientation of reservoir flow units as represented in engineering simulators of the Arab reservoirs correspond closely to the facies distribution implied by parasequences. This apparent relationship has not been fully-utilized in the characterization of Arabian Gulf reservoirs. Vertical permeability barriers and horizontal super-permeability channels, for example, can potentially be explained, correlated and mapped in terms of a parasequence framework. However, such a framework would only account for depositional and early diagenetic factors. A more comprehensive reservoir model would also require the incorporation of late diagenetic overprint and structural features, such as faults and fractures.

ACKNOWLEDGMENTS

The authors wish to thank the management of ADNOC, ADMA-OPCO and Halliburton Energy Services for their support and permission to publish. Special thanks are also extended to colleagues for their constructive discussions and suggestions. Strontium isotope analysis was performed by Isotopic Analytical Services Ltd., UK, under the supervision of Dr. John McBride. C / O and S isotope analyses and SEM photography were performed by the Russian Academy of Sciences, Russia, under the supervision of Dr. E.G.Morgun. XRD analysis was performed by the University of Durham, UK, under the supervision of Dr. M.E. Tucker. Funding for geochemical analyses was provided by Exxon Production Research Co. and Mobil Exploration and Production Corporation. Ross Peebles would like to thank Halliburton Energy Services for providing the time and resources necessary to conduct this research. The authors would like to thank Dr. Moujahed I. Al Husseini and Dr. Joerg Mattner and the anonymous referees, for their time and effort to edit this paper. Their suggestions, editing and redrafting of the figures in color have greatly improved the manuscript.

REFERENCES

Al-Silwadi, M.S., A. Kirkham, M.D. Simmons and B.N. Twombley 1996. *New Insights into Regional Correlation and Sedimentology, Arab Formation (Upper Jurassic), Offshore Abu Dhabi.* GeoArabia, v. 1, no. 1, p. 6-27.

Allen, J.R. and W.D. Wiggins 1993. *Dolomite Reservoirs: Geochemical Techniques for Evaluating Origin and Distribution.* American Association of Petroleum Geologists, Tulsa, 129 p.

Azer, S. 1989. *Preliminary Investigations into Possible Stratigraphic Traps, Offshore Abu Dhabi.* Paper presented at MEOS in Bahrain, SPE no. 17999, p. 739-753.

Claypool, C.F., W.T. Hosler, I.R. Kaplan, H. Sakai and L. Zak 1980. *The Age Curves of Sulphur and Oxygen in Marine Sulphates and their Mutual Interpretation.* Chemical Geology, v. 28, p. 199-260.

Goldhammer, R.K., P.J. Lehmann and P.A. Dunn 1993. *The Origin of High Frequency Platform Carbonate Cycles and Third-order Sequences (Lower Ordovician El Paso Group, West Texas): Constraints from Outcrop Data and Stratigraphic Modeling.* Journal of Sedimentary Petrology, v. 63, no. 3, p. 318-359.

Hosler, W.T., M. Scdidlowski, F.T. Mackenzie and J.B. Maynard 1988. *Geochemical Cycles of Carbon and Sulphur.* In C.B. Gregor, R.M. Garrels, F.T. Mackenzie and J.B. Maynard (Eds.), Chemical Cycles in the Evolution of the Earth. Wiley & Sons, New York, p. 105-174.

La Pointe, P. and H. Karakhanian 1990. *Sedimentology and Diagenesis: Basic Keys to Reservoir Layering - Example of the Umm Shaif Arab Zone C Reservoir.* Paper presented at the ADNOC / SPE Abu Dhabi Petroleum Conference, May 1990. SPE no. 305, p. 132-145.

Le Nindre, Y.M., J. Manivit, H. Manivit and D. Vaslet 1990. *Stratigraphie Sequentielle du Jurassique et du Cretace en Arabie Saoudite.* Geological Society of France Bulletin, v. 8, no. 6, p. 1025-1034.

De Matos, J.E. 1994. *Upper Jurassic-Lower Cretaceous Stratigraphy: The Arab, Hith and Rayda Formations in Abu Dhabi.* In M.D. Simmons (Ed.), Micropalaeontology and Hydrocarbon Exploration in the Middle East. Chapman & Hall, London, p. 81-101.

Moore, C.H. 1989. *Carbonate Diagenesis and Porosity Developments.* Sedimentology 46, Elsevier, Amsterdam, 338 p.

Morrow, D.W. 1982. *Diagenesis 2. Dolomite-Part 2. Dolomitization Models and Ancient Dolostones.* Geoscience Canada, v. 9, p. 95-107.

Murris R.J. 1980. Middle East: Stratigraphic Evolution and Oil Habitat. American Association of Petroleum Geologists, v. 64, p. 597-618.

Peebles, R.G., M. Suzuki and M. Shanor 1995. *The Effects of Long-term Shallow-burial Diagenesis on Carbonate Evaporite Successions.* In M.I. Al-Husseini (Ed.), Middle East Petroleum Geosciences, GEO'94. Gulf PetroLink, Bahrain, v. 2, p. 761-769.

Tucker, M.E. 1993. *Carbonate Diagenesis and Sequence Stratigraphy.* In V.P. Wright (Ed.), Sedimentology Review, Blackwells, Oxford, p. 51-72.

Tucker, M.E. and V.P. Wright 1990. *Carbonate Sedimentology.* Blackwell Scientific Publications, Oxford, 482 p.

Vail, P.R., R.M. Mitchum Jr., R.G. Todd, J.M. Widmier, S. Thompson III, J.B. Sangree, J.N. Bubb and W.G. Hatfield 1977. *Seismic Stratigraphy and Global Changes in Sea Level.* In C.E. Payton (Ed.), Seismic Stratigraphy - Applications to Hydrocarbon Exploration. American Association of Petroleum Geologists Memoir 26, p. 49-212.

ABOUT THE AUTHORS

Samir R. Azer *is a Senior Geologist with the Abu Dhabi Marine Operating Company (ADMA-OPCO). Prior to joining ADMA-OPCO in 1982, Samir worked with Western Desert Operating Petroleum Company (WEPCO) in Egypt as Geologist and Development Geology Super-visor. He has a BSc in Geology and Chemistry from Alexandria University, Egypt (1967). He is a member of the AAPG and SPWLA. An area of particular interest to Samir is sequence stratigraphy.*

Ross G. Peebles *is Senior Geoscientist with Halliburton Energy Services. Worked with Halliburton Reservoir Description Services in Abu Dhabi from 1991 to 1993. He received his BSc in Geological Oceanography from the Florida Institute of Technology in 1985 and a MSc in Geoscience from the University of Texas at Dallas. Ross is currently investigating the deposition and diagenesis of carbonate-evaporite successions within a sequence stratigraphic framework as part of PhD research at the University of Durham, UK.*

Paper presented originally as Paper SPE 29799 at the 9th Middle East Oil Show, MEOS'95, 11-14 March, 1995. Subsequently released at the request of the authors by the Society of Petroleum Engineers for publication in *GeoArabia*.

Manuscript Received 29 June, 1997

Revised 13 May, 1998

Accepted 19 May, 1998